J. Electroanal. Chem., 187 (1985) 205–227
Elsevier Sequoia S.A., Lausanne – Printed in The Netherlands

KINETICS OF FILM-COATED ELECTRODES

EFFECT OF A FINITE MASS TRANSFER RATE OF SUBSTRATE ACROSS THE FILM–SOLUTION INTERFACE AT STEADY STATE

JOHNA LEDDY and ALLEN J. BARD

Department of Chemistry, University of Texas, Austin, TX 78712 (U.S.A.)

J.T. MALOY

Department of Chemistry, Seton Hall University, South Orange, NJ 07079 (U.S.A.)

J.M. SAVÉANT

Laboratoire d'Electrochimie de l'Universite de Paris 7, Equipe de Recherche Associee au CNRS (No. 309, Electrochimie Moleculaire), 2, place Jussieu, 75251 Paris Cedex 05 (France)

(Received 18th September 1984; in revised form 18th December 1984)

ABSTRACT

Previous models for describing the mediation kinetics of film-coated electrodes quantitatively are extended to account for a finite mass transfer rate of the substrate across the film–solution interface. Experimental data from polymer-coated rotating disk electrode experiments, analyzed by the extended model, provide evidence for finite interfacial mass transfer rates. Substrate size and charge contribute to this interfacial rate. Interfacial mass transfer resistance is more pronounced for polymerized films such as poly(vinyl ferrocene) and poly[$Ru(vbpy)_3]^{2+}$ than for highly swollen polymers which bind electroactive species, e.g., poly(lysine).

INTRODUCTION

Mediated electrochemical reactions at film-coated electrodes have been modeled by Andrieux et al. [1], and Anson et al. [2]. The model encompasses four processes which can limit the rate of the mediated oxidation or reduction of the solution–soluble substrate by electroactive moieties within the film. These four limiting processes are (1) the mass transfer of the substrate in the solution; (2) the rate of the cross exchange reaction between the film moieties and the substrate, (3) the diffusion of the substrate from the film–solution interface toward the electrode–film interface; and (4) the diffusion-like propagation of charge, or, alternatively, the diffusion of the active form of the mediator, from the electrode toward the solution. In this paper, a fifth possible rate determining process, the rate of mass transfer of the substrate across the film–solution interface, is incorporated into the earlier models [1]. Previous treatments of permeation kinetics [1–11], based on equilibrium mass

0022-0728/85/$03.30

transfer of the substrate across the film–solution interface, represent a special case of the extended model.

Finite rates of interfacial mass transfer have been considered in a variety of non-electrochemical systems. Mass transfer across an interface has been suggested as a rate-limiting step of intercalation reactions at a solid–liquid interface [12], in liquid–liquid extraction and chromatography, and in permeation of dyes [13,14]. Davies and co-workers [15,16] suspended polymers, approximately a monolayer thick, between two immiscible liquids and measured interfacial mass transfer rates of 10^{-4} cm/s. In electrochemical systems, Ikeda et al. [17] and Ohnuki et al. [18] have characterized polymer films which are impermeable to a substrate in solution. Impermeable films have inhibited corrosion of conductor [19] and semiconductor surfaces. However, as the models developed [1–11] and a variety of mediated and catalyzed reactions studied [17,18,20–37], interfacial mass transfer was treated solely as an equilibrium process.

Herein, the finite mass transfer rate of a solution-soluble substrate across the film–solution interface is treated in a derivation which follows the method and notation developed previously [1]. The cross exchange reaction between the active form of the film-bound mediator, Q, and the substrate, A, is treated as irreversible. At potentials where only the reduction of P is possible, the scheme for reaction with the substrate is

$$P + e^- \rightleftarrows Q$$

$$A + Q \xrightarrow{k_1} P + B$$

where k_1 is the rate constant for the irreversible cross exchange reaction. At more negative potentials, the direct reduction of A to B is possible under mass transport limiting conditions

$$A + e^- \rightarrow B$$

This reaction scheme applies when B is chemically unstable or when the direct reduction A to B is thermodynamically allowed at the potential at which Q is generated, but the electrode kinetics are so slow that the rate of mediation by P/Q is faster. Reversible cross exchange reactions [1c] and self-exchange reactions [2], as well as multi-step catalytic process [1e] have also been treated using the equilibrium interfacial condition.

The rate of the mediated reactions is expressed by a set of current densities (i.e., fluxes), each of which represents a possible rate determining process. Andrieux et al. [1b,e] express these as four steady state current densities, which are proportional to the following rates:

$i_A \propto$ the mass transfer rate of the substrate, A, in solution to a bare electrode
$i_S \propto$ the mass transfer rate of the substrate, A, in the film
$i_\Sigma \propto$ the effective charge transfer rate via the mediator, Q, in the film
$i_k \propto$ the rate of the cross exchange reaction between A and Q

In this work, we introduce an additional limiting flux represented by the current density, i_p,

$i_p \propto$ the mass transfer rate of the substrate, A, across the film–solution interface

The model is developed for steady state, plateau current densities at a rotating disk electrode (RDE). Two plateau current densities are possible. When the film is electroactive, the first wave (designated as i_1) is due solely to the Q-mediated reduction of A; when a second wave (designated as i_2) occurs, it is due to the direct reduction of A. When the film is not electroactive, only one wave (i_1) may be observed, corresponding to the direct reduction of A. The plateau current densities to be expected when mass transfer across the film–solution interface is a rate-limiting process, are presented for each of ten limiting cases originally proposed for the case of interfacial equilibrium [1a,b,d].

BOUNDARY VALUE PROBLEM

The problem is expressed in terms of the following variables [1]. Some of these terms and representative concentration profiles are illustrated in Fig. 1.

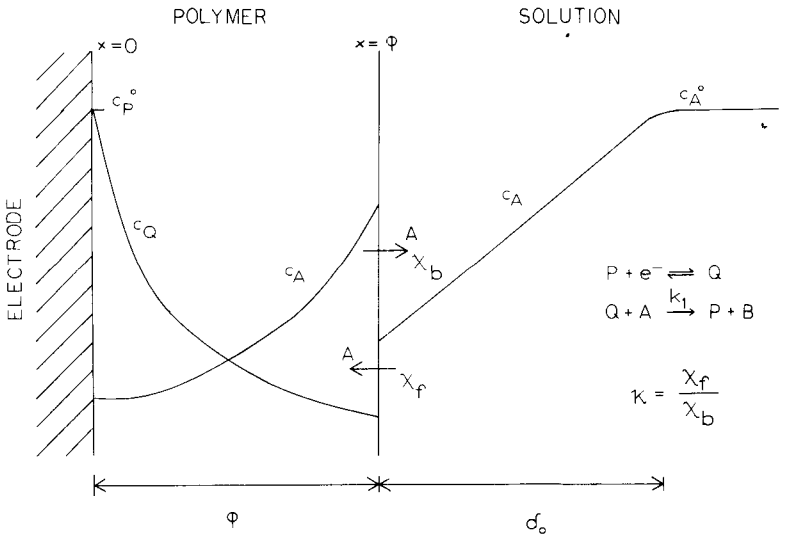

Fig. 1. The model system and parameters. Within the film of thickness ϕ the steady state concentration profiles for the active form of the mediator in the film, Q, and the substrate from the solution, A, are shown. The electrode is held at a potential such that all P (the inactive form of the mediator) which reaches the electrode surface is immediately reduced to Q; the concentration of Q at the electrode surface is, therefore, maintained at the maximum value, c_p°. Within the solution the concentration profile for A is approximately linear; δ_0 is the thickness of the diffusion layer. x is the coordinate normal to the electrode surface. χ_f and χ_b are the rate constants for the transport of A into and out of the film, respectively.

c_A°	bulk concentration of A in the solution
c_P°	Total concentration of the mediator in the film
Γ_m°	Surface concentration of the mediator, $\Gamma_m^\circ = c_P^\circ \phi$
c_Q, c_A	The steady state concentration of Q and A, respectively, dependent upon the distance normal to the electrode surface
D, D_S	Diffusion coefficient of A in the solution and the film, respectively
D_E	Effective diffusion coefficient for propagation of charge (Q) in the film
k_1	Rate of the cross exchange reaction
x	Coordinate normal to the electrode surface; $x = 0$ at the electrode–film interface
ϕ	Thickness of the film
δ	Thickness of the diffusion layer in the solution; $\delta = 4.98 D^{1/3} \nu^{1/6} \omega^{-1/2}$, for ω in rpm and ν in cm^2/s
χ_f, χ_b	Heterogeneous rate of mass transfer of A from the solution into the film and from the film into the solution, respectively
κ	Extraction coefficient; ratio of the initial concentration of A in the film and solution; $\kappa = \chi_f / \chi_b$
F	Faraday's constant
i	Plateau current density due to all electrochemical processes
i_1	Plateau current density of the first wave (due to the reduction of P to Q if the film is electroactive; if film electroinactive, due to reduction of A to B).
i_2	Plateau current density of second wave (due to the reduction of A to B if two waves are observed; then, $i_2 = i - i_1$).

The characteristic current densities expressed in terms of the above variables are:

$$i_A = F c_A^\circ D / \delta \tag{1}$$

$$i_S = F c_A^\circ \kappa D_S / \phi \tag{2}$$

$$i_E = F c_P^\circ D_E / \phi \tag{3}$$

$$i_k = F c_P^\circ c_A^\circ k_1 \phi \kappa \tag{4}$$

The newly defined interfacial current density, i_p, is:

$$i_p = F c_A^\circ \chi_f \tag{5}$$

Since the reaction between A and Q is chemically irreversible, only c_A and c_Q need to be considered in developing the mathematical model. The reaction between A and Q is confined to the film, where, under steady state conditions, these concentrations are obtained by solution of the following set of differential equations and boundary conditions.

$$D_E d^2 c_Q / dx^2 - k_1 c_Q c_A = 0 \tag{6}$$

$$D_S d^2 c_A / dx^2 - k_1 c_Q c_A = 0 \tag{7}$$

The boundary conditions for Q indicate that the electrode potential is sufficient to maintain the diffusion-limited reduction of P

$$c_Q(0) = c_P^\circ \tag{8}$$

where D_E is assumed to be identical for P and Q, and the mediator is confined to the film

$$\left.\frac{dc_Q}{dx}\right|_{x=\phi^-} = 0 \tag{9}$$

(The condition $x = \phi^-$ indicates the process is occurring on the film side of the film–solution interface, while ϕ^+ is associated with the solution side of the interface.)

The plateau current density due to both redox processes is given by

$$i = F\left[D_S \left.\frac{dc_A}{dx}\right|_{x=0} - D_E \left.\frac{dc_Q}{dx}\right|_{x=0}\right] \tag{10}$$

where the flux of Q is assumed to equal the flux of P at $x = 0$. The boundary conditions for A at the electrode–film interface depend upon the potential applied to the electrode. For potentials at which only direct reduction of P is possible

$$\left.\frac{dc_A}{dx}\right|_{x=0} = 0 \tag{11}$$

and the current density is given by

$$i = -FD_E \left.\frac{dc_Q}{dx}\right|_{x=0} \tag{12}$$

For potentials where the direct reduction of A is possible

$$c_A(0) = 0 \tag{13}$$

and the plateau current density is either given by eqn. (10) or by

$$i = FD_S \left.\frac{dc_A}{dx}\right|_{x=0} \tag{14}$$

which (in the event of electroinactivity of P or mediation by Q confined to a monolayer at the electrode surface) is obtained by allowing $D_E dc_Q/dx$ to approach zero in eqn. (10).

The boundary conditions for A at the film–solution interface are given in eqns. (15)–(17). The flux of A in the solution can be described by the approximation:

$$D \left.\frac{dc_A}{dx}\right|_{x=\phi^+} = \frac{D(c_A^\circ - c_A(\phi^+))}{\delta} \tag{15}$$

At steady state, the flux of A on either side of the interface must be equal to the net interfacial flux and, hence, these are equal to each other.

$$D_S \left.\frac{dc_A}{dx}\right|_{x=\phi^-} = \chi_f c_A(\phi^+) - \chi_b c_A(\phi^-) = D \left.\frac{dc_A}{dx}\right|_{x=\phi^+} \tag{16}$$

This boundary condition describes the finite rate of mass transfer across the film-solution interface and replaces the equilibrium condition employed previously

[1–11]

$$c_A(\phi^-) = \kappa c_A(\phi^+) \tag{17}$$

which is appropriate when mass transfer across the film-solution interface is fast compared to the other mass and electron transfer processes occurring within the film. When χ_f and $\chi_b \to \infty$, eqn. (16) simplifies to eqn. (17).

Under steady state conditions and linear mass transfer, the current density corresponding to the flux of material into the film at the film–solution interface given in eqn. (16) must equal the current density at the electrode surface given in eqn. (10). This yields

$$i = FD_S \left.\frac{dc_A}{dx}\right|_{x=\phi^-} = FD \left.\frac{dc_A}{dx}\right|_{x=\phi^+} \tag{18}$$

The solution of this boundary value problem requires that expressions be obtained for $c_A(\phi^+)$ and $c_A(\phi^-)$, the steady state interfacial substrate concentrations. In some instances (e.g., Case S), these expressions allow the solution to be obtained by algebraic manipulation. To obtain these expressions, we combine eqns. (1), (15), and (18)

$$c_A(\phi^+) = c_A^\circ\left(1 - i \cdot i_A^{-1}\right) \tag{19}$$

This relates the concentration of A just outside the film/solution interface to that in the bulk solution (c_A°). From eqns. (5), (16), and (19)

$$c_A(\phi^-) = c_A^\circ\kappa\left[1 - i\left(i_A^{-1} + i_p^{-1}\right)\right] \tag{20}$$

which relates the concentration of A just inside the film/solution interface to c_A°. This equation replaces

$$c_A(\phi^-) = c_A^\circ\kappa\left(1 - i \cdot i_A^{-1}\right) \tag{21}$$

which has been used in the development [1a] of the equilibrium model. Equation (20) arises from eqns. (17) and (19) under the condition of interfacial equilibrium. Thus, the interfacial equilibrium theory and equations can be employed once eqn. (21) has been substituted for eqn. (20).

PASSIVE FILMS: CASE S

The simplest case for this boundary value problem occurs when the film is electroinactive (i.e., $c_P^\circ = 0$ or $D_E = 0$). This case, identified as Case S [1a], was originally studied by Gough and Leypoldt [3] under conditions of interfacial equilibrium. In the following, Case S is used to illustrate both the solution of the problem and a method for determining the rate of interfacial mass transfer.

Within a passive film, the concentration of the substrate is not perturbed by a cross exchange reaction ($D_E dc_Q/dx \to 0$), and the concentration profile within the film is linear. The derivative in eqn. (14) can, therefore, be represented as the drop in substrate concentration over the film thickness. The concentration at the electrode

surface is zero, eqn. (13), and i is

$$i = FD_S c_A(\phi^-)/\phi = i_S c_A(\phi^-)/\kappa c_A^\circ \tag{22}$$

by combination with eqn. (2). Equations (20) and (22) yield i for Case S in terms of the characteristic current densities:

$$i^{-1} = i_A^{-1} + i_p^{-1} + i_S^{-1} \tag{23}$$

It is useful to note that eqn. (23) can also be obtained directly by observing that, for Case S at steady state, the flux through the film, the flux across the film/solution interface, and the flux to the film from solution are all equal to i/F. Hence, by eqns. (15), (16), and (22),

$$i/F = D_S c_A(\phi^-)/\phi = \chi_f c_A(\phi^+) - \chi_b c_A(\phi^-) = (D/\delta)[c_A^\circ - c_A(\phi^+)] \tag{24}$$

or in terms of the characteristic current densities of (eqns. 1, 2, and 5),

$$i = \frac{i_S}{\kappa c_A^\circ} c_A(\phi^-) = \frac{i_p}{c_A^\circ}\left[c_A(\phi^+) - \frac{c_A(\phi^-)}{\kappa}\right] = i_A\left[1 - \frac{c_A(\phi^+)}{c_A^\circ}\right] \tag{25}$$

The interfacial concentrations $c_A(\phi^+)$ and $c_A(\phi^-)$ may be readily eliminated from these three equations to obtain eqn. (23), upon which the interpretation of steady state Case S behavior is based. By assuming steady state behavior leading to linear concentration gradients, it is sometimes possible, as in this case, to employ simple algebraic manipulations to obtain the correct solution to the boundary value problem.

The interpretation of experimental Case S mechanistic behavior is made possible by the construction of a Koutecký–Levich plot which shows the variation of the reciprocal steady-state current observed at a modified electrode with that of the unmodified electrode at identical rotation rates. Since i_A^{-1} is the only variable in eqn. (23) that depends upon ω, the Koutecký–Levich plot is given by i^{-1} vs. i_A^{-1} and this variation is linear with a slope of unity and an intercept of $(i_p^{-1} + i_S^{-1})$. For the bare electrode, this intercept is zero because the current is limited solely by mass transport of substrate in solution ($i_p \to \infty$ and $i_S \to \infty$). For film-coated electrodes, this intercept increases with ϕ because i_S, the only ϕ-dependent term in eqn. (23), exhibits this dependence. Thus, a plot of the Koutecký–Levich intercept vs. ϕ is linear, yielding an intercept of i_p^{-1}. This observation provides a convenient diagnostic criterion for distinguishing interfacial mass transfer effects in Case S. When equilibrium occurs at the film/solution interface, $i_p \to \infty$ and the intercept of the Koutecký–Levich plot is i_S^{-1}. In the case of equilibrium, then, the variation of the Koutecký–Levich intercept should be linear with film thickness, exhibiting no intercept corresponding to i_p^{-1}. The relative importance of finite mass transfer across this interface can be assessed by considering the relative importance of i_p^{-1} and i_S^{-1}.

Rigorous solution of the general boundary value problem with similar considerations regarding the various kinetic limitations yields diagnostic criteria which may be applied in the other cases involving electroactive films. As in this Case S example,

this treatment results in formulating mechanistic criteria which are valid whenever the previously described steady state assumptions are valid.

ELECTROACTIVE FILMS — HOMOGENEOUS MEDIATED REACTIONS

The solution of the general boundary value problem is strictly analogous to that presented previously [1a] wherein the system of differential equations described above was reduced to a single equation

$$(d^2a/dy^2) - (i_k/i_s)a[1 + (i_S/i_E)(a - a_0 - y(da/dy)_1)] = 0 \tag{26}$$

in the two dimensionless parameters $a = c_A/\kappa c_A^\circ$ and $y = x/\phi$. The boundary condition $a_0 = 0$ was employed when A is electroactive and $da/dy|_0 = 0$ when only P is electroactive. Since $a_{1-} = c_A(\phi^-)/\kappa c_A^\circ$, the equilibrium boundary condition, eqn. (21), is expressed as

$$a_{1-} = 1 - (i/i_A) \tag{27}$$

Under steady-state conditions of a finite, interfacial mass transfer rate, this boundary condition is replaced with eqn. (20),

$$a_{1-} = 1 - i[(1/i_A) + (1/i_p)] \tag{28}$$

These two equations are the only difference in the boundary conditions required to treat the two cases. Since i_A and i_p are both unspecified constants, it is not surprising that all of the solutions given previously [1a,b] are applicable in the case of interfacial mass transfer control, provided that i_A^{-1} in these previous treatments is replaced with $(i_A^{-1} + i_p^{-1})$.

To demonstrate this formally, it is convenient to cast these equations in the formalism in which the concentration of A is normalized with respect to the concentration at the film/solution interface, $c_A(\phi^-)$; see eqn. (20).

$$a^* = c_A/c_A(\phi^-) = c_A/\kappa c_A^\circ[1 - i(i_A^{-1} + i_p^{-1})] = a/[1 - i(i_A^{-1} + i_p^{-1})] \tag{29}$$

This has the advantage of allowing the system of equations to be described completely by the same equation as previously given [1d], which may be obtained by substituting eqn. (29) into eqn. (26)

$$(d^2a^*/dy^2) - (i_k^*/i_S^*)a^*\{1 + (i_S^*/i_E)[a^* - a_0^* - y(da^*/dy)_1]\} = 0 \tag{30}$$

with

$$i_S^* = i_S[1 - i(i_A^{-1} + i_p^{-1})] \tag{31}$$

and

$$i_k^* = i_k[1 - i(i_A^{-1} + i_p^{-1})] \tag{32}$$

rather than those previously employed. The boundary conditions then become $a_1^* = 1$ and $da^*/dy|_0 = 0$ at the first wave and $a_0^* = 0$ at the second wave. By combining eqns. (2), (18), (29) and (31) an expression for the current density may be

obtained as

$$i = i_S^* \, (\mathrm{d}a^*/\mathrm{d}y)|_1 \tag{33}$$

Again, the term i_A^{-1} in the interfacial equilibrium equations is replaced by $[i_A^{-1} + i_p^{-1}]$ to obtain eqns. (31) and (32). This demonstrates rigorously that, in all cases, the expressions for the limiting current densities can be derived from the expressions for the case of interfacial equilibrium simply by replacing i_A^{-1}.

Since equations of the same form arise in this treatment of the steady state effects of interfacial mass transfer, the results may be described in the formalism developed for the equilibrium condition. In that work, each of the limiting cases was designated by a combination of the letters, E, R, and S [1a]. The letters indicate a mass or an electron transfer process that is sufficiently slow to control the net rate of the mediated reactions and, thus, the magnitude of the plateau current densities. The rate limiting processes corresponding to these letters are

E Charge propagation (via the P/Q couple) through the film
R The cross exchange reaction
S The mass transfer of the substrate (A) within the film

Each case designation depends upon the relative magnitude of the five characteristic currents i_k, i_S, i_E, i_A, and i_p, all of which are included in the currents defined as i_S^*, i_k^* and i_E. These designations and the expected plateau current densities for each case are listed in Table 1. Those cases where a linear Koutecký–Levich plot is expected are indicated by †. The factors governing the passage between the various limiting situations are best seen on the kinetic zone diagram shown in Fig. 2. In spite of the large number of experimental parameters governing the system, only two dimensionless parameters i_S^*/i_k^* and i_E/i_k^* [which appear in eqn. (30) as coefficients i_k^*/i_S^* and $i_S^*/i_E = (i_S^*/i_k^*)/(i_E/i_k^*)$] are necessary to determine the case designation when the steady state condition is satisfied. For example, Case R is shown in Fig. 2 to result whenever both i_S^*/i_k^* and i_E/i_k^* exceed 10, regardless of whether this occurs because i_S^* and/or i_E are large or i_k^* is small. On the other hand, as both i_S^*/i_k^* and i_E/i_k^* approach zero, a variety of case designations are possible, depending upon the relative magnitudes of i_S^*, i_E, and i_k^*. That is, when i_k^* is large, Case S + E results when $i_S^* \simeq i_E$; Case S results when $i_S^* > i_E$; and Case E results when $i_S^* < i_E$. Note that these case designations are independent of the individual rate expressions contributing to the magnitude of i_S^* and i_k^*. Thus, i_k^* may be "large" (as large as i_k) when *both* i_A and i_p are large, but i_k^* approaches zero as *either* i_A or i_p becomes rate-determining. Thus, both i_A and i_p contribute in the same manner to case designation, and in this respect are indistinguishable; only in the subsequent interpretation of the data (by the criteria developed herein) would the relative magnitudes of i_A and i_p become important. That only a two-dimensional representation is necessary to characterize behavior which may be controlled by as many as five characteristic currents can be attributed to the fact that only two variable coefficients appear in eqn. (30) and these may each be expressed in terms of the two variables appearing in the zone diagram in Fig. 2.

TABLE 1

Expressions of the plateau currents

(R+S)

$$\dagger \quad \frac{1}{i_1} = \frac{1}{i_A} + \left\{ \frac{1}{i_p} + \frac{1}{(i_k i_S)^{1/2} \tanh\left(\frac{i_k}{i_S}\right)^{1/2}} \right\}$$

$(m) = 1$

$$\dagger \quad \frac{1}{i_1 + i_2} = \frac{1}{i_A} + \left\{ \frac{1}{i_p} + \frac{\tanh\left(\frac{i_k}{i_S}\right)^{1/2}}{(i_k i_S)^{1/2}} \right\}$$

$(m) = 1$

(R)

$$\dagger \quad \frac{1}{i_1} = \frac{1}{i_A} + \left\{ \frac{1}{i_p} + \frac{1}{i_k} \right\}$$

$(m) = 1 \qquad (b) = (Fc_p^\circ c_A^\circ k_1 \kappa \phi)^{-1} + i_p^{-1}$

$$\dagger \quad \frac{1}{i_1 + i_2} = \frac{1}{i_A} + \left\{ \frac{1}{i_p} + \frac{1}{i_S} \right\}$$

$(m) = 1 \qquad (b) = \phi / Fc_A^\circ \kappa D_S + i_p^{-1}$

(E+R)

$$\frac{1}{i_1} = \frac{1}{i_A} + \frac{1}{i_p} + \frac{i_1}{i_k i_E \tanh^2\left\{ \frac{i_k}{i_E}\left[1 - i_1\left(\frac{1}{i_A} + \frac{1}{i_p}\right)\right]\right\}^{1/2}}$$

$$\dagger \quad \frac{1}{i_1 + i_2} = \frac{1}{i_A} + \left\{ \frac{1}{i_p} + \frac{1}{i_S} \right\}$$

$(m) = 1 \qquad (b) = \phi / Fc_A^\circ \kappa D_S + i_p^{-1}$

(SR)

$$\dagger \quad \frac{1}{i_1} = \frac{1}{i_A} + \left\{ \frac{1}{i_p} + \frac{1}{(i_k i_S)^{1/2}} \right\}$$

$(m) = 1 \qquad (b) = 1 / Fc_A^\circ \kappa (c_p^\circ D_S k_1)^{1/2} + i_p^{-1}$

$i_2 = 0$

General case

$$i = i_S^*\left(\frac{da^*}{dy}\right)_1$$

Numerical resolution of eqn. (30) with $a_1^* = 1$ and $(da^*/dy)_0 = 0$ at the first wave and $a_0 = 0$ at the second wave

(ER)

$$\P \quad \left[\frac{1}{i_1} - \frac{1}{i_A}\right] = \left\{\frac{1}{i_p}\right\} + \frac{i_1}{\{i_k i_E\}}$$

$(m) = (i_k i_E)^{-1} \qquad (b) = i_p^{-1}$

$$\dagger \quad \frac{1}{i_1 + i_2} = \frac{1}{i_A} + \left\{ \frac{1}{i_p} + \frac{1}{i_S} \right\}$$

$(m) = 1 \qquad (b) = \phi / Fc_A^\circ \kappa D_S + i_p^{-1}$

$$\frac{1}{i_1} = \frac{1}{i_A} + \frac{1}{i_p} + \frac{1}{\left[i_k i_S \left(1 - \frac{i_1}{i_E} \right) \right]^{1/2}}$$

$i_2 = 0$

(SR + E)

† Exhibits linear Koutecký–Levich behavior with (m) = slope and (b) = intercept

¶ Non-linear Koutecký–Levich behavior, but a linear form is given having (m) = slope and (b) = intercept
$i_p^{-1} = 1/Fc_A^\circ \chi_f$

¶ $$\left[\frac{1}{i_1} - \frac{1}{i_A} \right] = \left\{ \frac{1}{i_p} + \frac{1}{i_S} \right\} + \frac{i_1}{\{ i_k i_E \}}$$

$(m) = (i_k i_E)^{-1}$ $\quad (b) = \phi / Fc_A^\circ \kappa D_S + i_p^{-1}$

† $$\frac{1}{i_1 + i_2} = \frac{1}{i_A} + \left\{ \frac{1}{i_p} + \frac{1}{i_S} \right\}$$

$(m) = 1$ $\quad (b) = \phi / Fc_A^\circ \kappa D_S + i_p^{-1}$

(ER + S)

† $$\frac{1}{i_1} = \left\{ \frac{1}{i_E} \right\}$$

$(m) = 0$ $\quad (b) = i_E^{-1}$

$i_2 = 0$

(E)

† $$\frac{1}{i_1} = \left\{ \frac{i_S}{i_S + i_E} \right\} \frac{1}{i_A} + \left\{ \frac{1}{i_S + i_E} \left(1 + \frac{i_S}{i_p} \right) \right\}$$

$(b)/(m) = \phi / Fc_A^\circ \kappa D_S + i_p^{-1}$

$i_2 = 0$

(S + E)

† $$\frac{1}{i_1} = \frac{1}{i_A} + \left\{ \frac{1}{i_p} + \frac{1}{i_S} \right\}$$

$(m) = 1$ $\quad (b) = \phi / Fc_A^\circ \kappa D_S + i_p^{-1}$

$i_2 = 0$

(S)

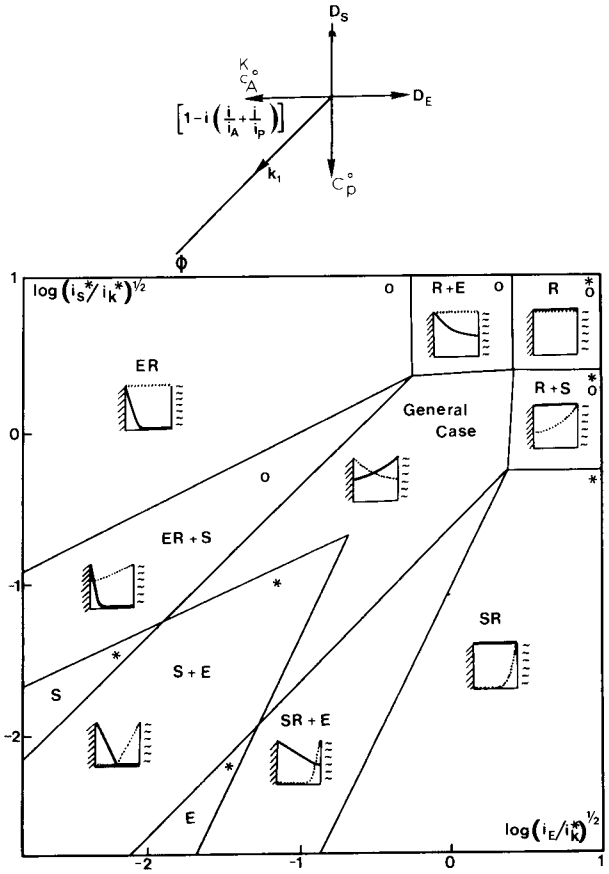

Fig. 2. Zone diagram. (*) Linear Koutecký–Levich plots; (O) second wave.

ELECTROACTIVE FILMS. SURFACE MEDIATED REACTIONS

In the "SR + E" and "ER + S" cases, when the mediation reaction is so fast that the corresponding reaction layers, located respectively at the film–solution and film–electrode boundaries, are so thin as to involve a single monolayer of mediator, the R reaction then becomes a surface reaction [1,9]. The "Sr + E" and "Er + S" kinetic situations are then obtained, the lower case letter r symbolizing the surface character of the R reaction. With the same method as previously described, the following expressions are obtained: "Er + S" (mediation reaction occurring at the electrode–film interface):

$$1/i_1 = 1/i_A + 1/i_p + 1/i_S + 1/i_k \tag{34}$$

$$1/(i_1 + i_2) = 1/i_A + 1/i_p + 1/i_S \tag{35}$$

"Sr + E" (mediation reaction occurring at the film–solution interface):

$$1/i_1 = 1/i_A + 1/i_p + 1/i_k\left[1 - (i_1/i_E)\right] \tag{36}$$

$$i_2 = 0 \tag{37}$$

i_k being now a characteristic charge density for a surface reaction:

$$i_k = F\kappa k_m c_A^\circ \Gamma_m^\circ \tag{38}$$

(where k_m = rate constant in a monolayer, Γ_m° = monolayer surface concentration of the mediator).

In the "Sr + E" case, it is found that the penetration reaction interferes through its equilibrium and kinetic characteristics simply because this was built into the model. In a number of circumstances, this will not have practical significance, since one can regard a monolayer of catalyst deposited on the electrode as being freely accessible by the substrate, which would correspond to $\kappa = 1$ and $\chi_f \to \infty$. However, where the reaction between A and Q requires a precursor complex to be formed (equilibrium constant κ, forward rate constant χ_f) eqns. (36)–(38) would then represent the resulting electrochemical kinetics.

DIAGNOSTIC CRITERIA

In addition to providing the plateau current densities, Table 1 indicates the diagnostic criteria by which experimental data may be treated in order to assess the effect of interfacial mass transfer resistance in each of the cases developed previously under equilibrium conditions. In general, this mechanistic diagnosis begins with the construction of a Koutecký–Levich plot. In all cases except SR + E, linear Koutecký–Levich behavior is predicted for at least one of the observed waves, and in only three other cases (the first waves of E + R, ER, and ER + S) is non-linear Koutecký–Levich behavior predicted for one of the waves. Even in two of these cases (ER and ER + S) linear diagnostic plots may be obtained by constructing $(i_1^{-1} - i_A^{-1})$ vs. i_1 plots. Interfacial mass transfer effects may be assessed through variations in the slope (m) and the intercept (b) of these linear diagnostic plots under changing experimental conditions.

For example, examination of Table 1 reveals that, quite often, $(m) = 1$; in Koutecký–Levich plots, this indicates that there is no limitation due to electron propagation within the film [34]. Thus, for a linear plot the observation of $(m) = 1$ immediately rules out those cases (E, S + E) in which some limitations by charge propagation within the film exist. While this sort of information is quite useful in mechanistic determination, (m) is generally independent of interfacial mass transfer effects. Thus, the determination of i_p^{-1} depends upon the evaluation of (b). In many of the cases appearing in Table 1, for example, $(b) = (\phi/Fc_A^\circ \kappa D_S) + i_p^{-1}$. To utilize this diagnostic, one must vary the experimental conditions so as to determine i_p^{-1} through variations in (b). Since $i_p^{-1} = 1/Fc_A^\circ \chi_f$, the only experimental variable that will produce a change in (b) in these cases without causing a similar change in i_p^{-1} is

the film thickness, ϕ. Therefore, the indicated diagnostic is the construction of the (b) vs. ϕ plot to obtain the intercept i_p^{-1}. In the event of rapid interfacial mass transfer kinetics, $i_p \rightarrow \infty$ and the (b) vs. ϕ plot will pass through the origin.

In practice it is sometimes convenient to construct modified Koutecký–Levich plots of Fc_A°/i vs. Fc_A°/i_A. For Case S, the intercepts of these plots, Fc_A° (b), when plotted against ϕ, yield a straight line which has an intercept of $Fc_A^\circ i_p^{-1} = \chi_f^{-1}$ and a slope of $1/(\kappa D_S)$. (This technique was used in the interpretation of the data appearing in Fig. 3, below.) In the event that ϕ cannot be measured directly, it is also valid to plot (b) or Fc_A° (b) against Γ_m°, a quantity that is directly proportional to ϕ, so long as c_p° remains constant. In this instance, the interpretation of χ_f from the intercept of (b) or Fc_A° (b) vs. Γ_m° remains the same, but the slope interpretation must be modified to account for the (unknown) constant c_p°. Thus, in the Case S plots of Fc_A° (b) vs. Γ_m° reported herein (Figs. 4 and 5), the intercept is χ_f^{-1}, while the slope yields $1/(\kappa c_p^\circ D_S)$. The results of this sort of analysis appears in Table 2.

Similar data analysis strategies must be developed for each of the cases shown in Table 1 in which (b) depends upon i_p^{-1}. Generally, this will be accomplished through the determination of the direct variation of intercept with film thickness, but there are cases where (b) exhibits ϕ^{-1}-dependence (R), where (b) exhibits no ϕ-dependence (SR), and where (b) is independent of i_p (E). In one instance (E + R), the intercept of the linear diagnostic plot yields i_p^{-1} directly. Whatever data analysis strategy is developed, however, it is important to keep in mind that variations in experimental parameters such as ϕ and c_p° change the prevailing limiting conditions leading to the various case designations. Thus, some care must be exercised to assure that these experimental variations do not cause a change in the appropriate theoreti-

TABLE 2

Summary of data taken from the literature and analyzed for a finite rate of mass transfer across the polymer–solution interface (All are Case S. All are analyzed at Pt in MeCN unless otherwise noted.)

Polymer	Substrate	Ref.	χ_f ($= i_p/Fc_A^\circ$)/ cm s^{-1}	$\kappa c_p^\circ D_s$ ($= i_S\Gamma_T/Fc_A^\circ$)/ mol cm^{-1} s^{-1}	$\kappa c_p^\circ D_S$ [a]
PVF	BQ	31	0.1	7.8×10^{-9}	1.3×10^{-9}
Poly[VDQ]$^{2+}$	Fer	33	0.01	3.5×10^{-12}	2.2×10^{-12}
Poly[Ru(bpy)$_2$(p-cinn)$_2$]$^{2+}$	Fer	33	>1.1	1.3×10^{-10}	1.2×10^{-10}
	$Ru(bpy)_2Cl_2$	33	0.05	2.0×10^{-11}	1.3×10^{-11}
Poly[Ru(vbpy)$_3$]$^{2+}$	BQ	33	[b]	7.0×10^{-11}	8.7×10^{-11}
	Fer	32	0.01 ± 0.005	5.6×10^{-8}	4.3×10^{-8}
PLC/$Mo(CN)_8^{3-}$ [c]	$Co(tpy)_2^{2+}$	30	[b]	7.5×10^{-10}	7.9×10^{-10}
PLL/$Co(C_2O_4)_3^{2-}$ [c]	$Co(C_2O_4)_3^{2-}$	37	[b]	1.3×10^{-8}	1.3×10^{-8}

[a] Value found without accounting for a finite interfacial mass transfer rate, as reported in the reference.
[b] intercept (b) vs. Γ_T has a negative intercept, suggesting interfacial mass transport is not a current limiting process.
[c] pH = 5.5, with 0.2 M acetate buffer.

cal development to be used in the analysis. In this regard, it is useful to observe that in four of the five cases where a second wave is possible, $(i_1 + i_2)^{-1} = i_A^{-1} + i_p^{-1} + i_S^{-1}$, and variations among these cases (R, E + R, ER, and ER + S), brought about by changes in ϕ, are of no consequence in determining i_p^{-1}. This observation suggests that steady state current measurements on the second plateau, if possible, are most appropriate for the determination of i_p^{-1}. However, this determination also requires the variation in ϕ in a reproducible manner.

For some of the limiting cases, comments regarding the results summarized iin Table 1 are required:

(1) E: i_1 is independent of i_p (and i_A).

(2) S: $i_1^{-1} = i_A^{-1} + i_p^{-1} + i_S^{-1}$. Note that in ref. 1b, Table 1, Case S should read $i_1^{-1} = i_A^{-1} + i_S^{-1}$.

(3) R + S yields a linear Koutecký–Levich plot for both i_1 and $i_1 + i_2$ but no linear plot of (b) as a function of ϕ or c_p° is possible because these variables are related to i_1 and $i_1 + i_2$ through the hyperbolic tangent.

(4) SR: The Koutecký–Levich plot is linear, but $(b) = (i_k i_S)^{-1/2} + i_p^{-1}$ has no dependence on ϕ. i_p can only be found if c_p° can be varied without affecting ϕ or D_S.

(5) R + S and SR + E: For these two cases, no linear relationship exists between i_p and ϕ for either i_1 or $i_1 + i_2$.

(6) ER: i_p^{-1} is determined directly from the (b) of $(i_1^{-1} - i_A^{-1})$ vs. i_1; no second plot is required.

(7) R + E: No linear analysis for i_p is available using i_1; the analysis based on $i_1 + i_2$ is straightforward, however.

(8) ER, ER + S: The necessity of determining i_S from measurements made with an inert substrate in order to identify the characteristic current densities is eliminated in these two cases by plotting $i_1^{-1} - i_A^{-1}$ vs. i_1.

(9) SR + E: If $i_p^{-1} = 0$, then a plot of $(i_1^{-1} - i_A^{-1})^{-2}$ vs. i_1 will be linear with $(m) = -i_k i_S / i_E$ and $(b) = i_k i_S$.

(10) R + E, R, ER, and ER + S: $(i_1 + i_2) = i_A^{-1} + i_p^{-1} + i_S^{-1}$. This expression for the plateau current is the same as i_1 for case S; the plateau current is limited only by the mass transfer of A in the solution (i_A), across the film-solution interface (i_p) and through the film (i_S).

(11) S, S + E, E, SR, R + S, R: The gradient of Q is a constant across the film, and as a result, the Koutecký–Levich plots for the first wave are linear.

(12) R + E, ER + S, ER, and SR + E are limited by i_k and i_E. (The case designation contains both E and R.) In each case the expression for the plateau current contains i_1 on both sides of the equation; this is also true of $i_1 + i_2$ for Case SR + E.

Mediated reactions which occur in a monolayer at the electrode/film (Er + S) and film/solution (Sr + E) interface are two additional cases to consider. The expressions for the plateau current densities are presented in eqns. (34) to (39). Er + S arises when the concentration of Q is confined to a monolayer at the electrode surface, i.e., the electrons are unable to propagate through the film. Two waves can be observed for Er + S, and both yield linear Koutecký–Levich plots. The

separation of i_k from i_p cannot be effected through measurements of i_1 because i_k is no longer ϕ-dependent. However, $i_1 + i_2$ can be used to determine i_p, and, then, i_k can be extracted from i_1 (eqns. 34 and 35).

Case Sr + E arises when the substrate is unable to penetrate the film. No second wave is observed in this case, and a linear Koutecký–Levich plot is obtained only when $i_E \gg i_1$ (Eqn. 36). In this case $(b) = i_p^{-1} + i_k^{-1}$, and, again, in an interfacial reaction, these characteristic current densities cannot be separated. The various limiting cases for the Sr + E and Er + S cases can also be considered using the i_k^* and i_S^* formalism of eqns. (31) and (32). Then

Er + S

$$1/i_1 = 1/i_k^* + 1/i_S^* \tag{39}$$

For the two limiting cases

$i_k^*/i_S^* \to 0$ (Case Er)

$$1/i_1 = 1/i_k^* = 1/i_k + 1/i_p + 1/i_A \tag{40}$$

$i_k^*/i_S^* \to \infty$ (Case S)

$$1/i_1 = 1/i_S^* = 1/i_S + 1/i_p + 1/i_A \tag{41}$$

Sr + E

$$1/i_1 = 1/i_k^* + 1/i_E^* \tag{42}$$

For the two limiting cases

$i_k^*/i_E^* \to 0$ (Case Sr)

$$1/i_1 = 1/i_k^* = 1/i_k + 1/i_p + 1/i_A \tag{43}$$

$i_k^*/i_E^* \to \infty$ (Case E)

$$1/i_1 = 1/i_E \tag{44}$$

In Case Sr + E, where the reaction occurs in a monolayer at the film/solution interface, a finite value of i_p can be interpreted as the rate of some process which must occur before the electron transfer, i.e., the formation of a precursor state at the film surface.

EXPERIMENTAL

Case S studies

The question of a finite rate of mass transfer across the film/solution interface arose in a study of the permeability of poly(vinyl ferrocene), PVF, on platinum to

benzoquinone, BQ. The measurements were made in 0.1 M $TBABF_4$ in acetonitrile (MeCN) as discussed previously [31]. Koutecký–Levich plots for the one-electron reduction of BQ are shown in Fig. 3 for several thicknesses of PVF. The slope for each thickness is the same as that for the bare electrode; mediation is precluded, because PVF is electroinactive at the potentials employed. Thus, these data are characterized as strictly Case S. As discussed previously, i_p is determined by plotting (b) vs. ϕ (Fig. 3b). The intercept of this second plot indicates $\chi_f \sim 0.1$ cm/s, $[i_p/Fc_A^\circ = \chi_f]$, and the slope yields $D_S = 2.4 \times 10^{-6}$ cm^2/s, $[i_S/Fc_A^\circ = \kappa D_S/\phi]$. Based on an analysis which assumes mass transfer across the film–solution interface is an equilibrium process, D_S would be 4×10^{-7} cm^2/s [31].

We have examined several previous reports of permeation of substrate through a polymer film (Case S), looking for evidence of slow interfacial mass transport. Murray and co-workers [32,33] studied the permeation of a number of substrates with several polymers which were deposited on a platinum surface by electropolymerization of the monomer. The studies were made in 0.1 M Et_4NClO_4/MeCN, with the polymers poly$[VDQ]^{2+}$, poly$[Ru(vpby)_3]^{2+}$, and poly$[Ru(bpy)_2(p\text{-cinn})_2]^{2+}$. ($VDQ^{2+}$ = vinyl diquat; vbpy is a vinyl analog of bpy = 2,2′-bipyridine; p-cinn = N-(4-pyridine)cinnamamide.) For these polymers and a variety of substrates, plots of Fc_A° (b) vs. Γ_m° are shown in Fig. 4. The values found for χ_f are summarized in Table 2; the values determined for $c_p^\circ \kappa D_S$, with and without account of interfacial resistance, are also cited. Mass transfer of ferrocene, Fer, across the film–solution interface of poly$[VDQ]^{2+}$ is characterized by an interfacial rate constant of 10^{-2}

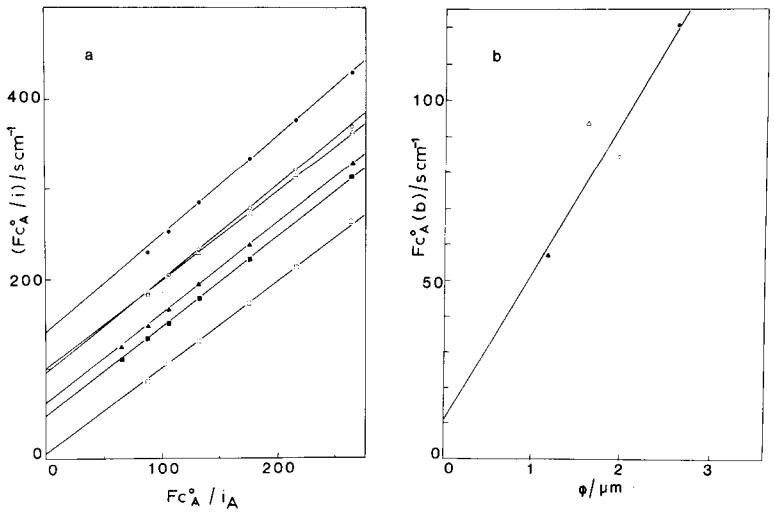

Fig. 3. (a) Koutecký–Levich plots for the reduction of BQ at a bare platinum electrode (□) and five PVF-modified electrodes, each of a different thickness; the thicknesses are (■) 2.61, (▲) 1.96, (△) 1.61, (○) 1.19, (●) 0.82 μm. The slopes of the PVF-modified electrodes and the bare electrode are the same within 10%. (b) Plot of the intercepts in (a) as a function of thickness. The intercept of this plot, equal to $i_p^{-1} = F\chi_f c_A^\circ$, yields $\chi_f \sim 0.1$ cm/s.

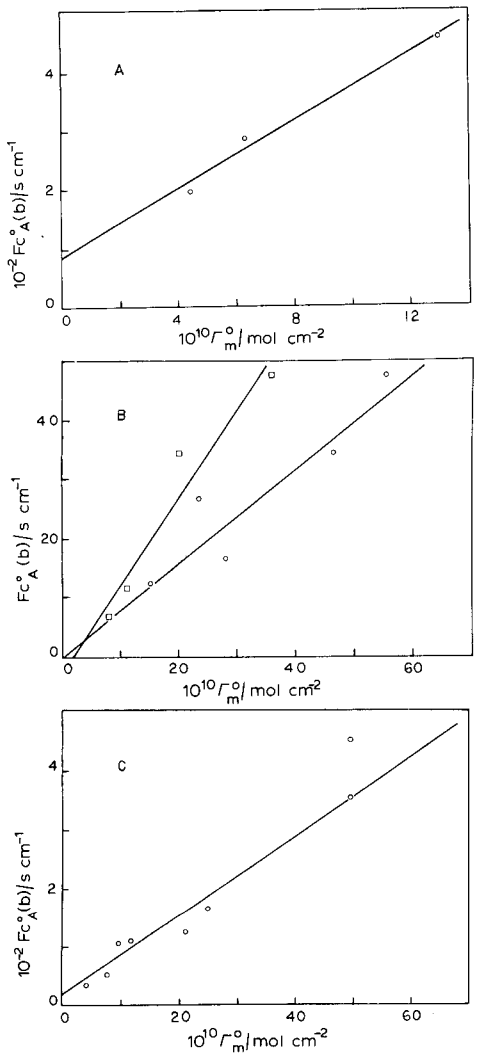

Fig. 4. Plots analogous to those in Fig. 3b, for a variety of polymers and substrate are shown for Case S. The slopes are proportional to i_S^{-1} and the intercepts are proportional to i_p^{-1}. (a) Ferrocene through poly[VDQ]$^{2+}$; (b) BQ through poly[Ru(vbpy)$_3$]$^{2+}$ (□) and ferrocene through poly[Ru(bpy)$_2$(p-cinn)$_2$]$^{2+}$ (○). (c) Ru(bpy)$_2$Cl$_2$ through poly[Ru(bpy)$_2$(p-cinn)$_2$]$^{2+}$. The data was taken from ref. 33.

cm/s (Fig. 4a); the value found for poly[Ru(bpy)$_2$(p-cinn)$_2$]$^{2+}$ and the same substrate [33] is > 1.1 cm/s (Fig. 4b). Only a lower limit can be given for the latter, because the value found for $c_p^{\circ}\kappa D_S$ is essentially the same whether account is taken of i_p or not. For the same polymer (Fig. 4c), however, an interfacial rate constant of 0.05 cm/s was found for Ru(bpy)$_2$Cl$_2$ [33]. The final polymer in this series is

poly[Ru(vbpy)$_3$]$^{2+}$ [32,33]. The data for some of the substrates examined were too scattered to evaluate χ_f. The BQ data, however, yielded a linear plot of Fc_A° (b) vs. Γ_m°, as shown in Fig. 4b. The intercept was slightly negative, suggesting slow interfacial transport is not a current limiting process. A χ_f-value of 0.01 cm/s was found from a similar plot for ferrocene. The value found for i_S is 30% higher when interfacial resistance is taken into account than when it is not.

The interfacial resistances found for the remaining two systems, involving aqueous solutions, are negligible. The permeation of Co(tpy)$_2^{2+}$ (tpy = 2,2′,2-terpyridine) through a poly-L-lysine copolymer (PLC) with incorporated Mo(CN)$_8^{3-}$ on pyrolytic graphite was examined through its direct oxidation [29]. The thickness and structure of the film was found to change with the amount of incorporated Mo(CN)$_8^{3-}$, and the analysis of i_p is based on three thicknesses for which $\Gamma_{PLC}/\Gamma_{Mo(CN)_8^{3-}} = 8$. Protonated poly(lysine) PLL, with the substrate Co(C$_2$O$_4$)$_3^{3-}$ (0.5 mM) was also examined for three thicknesses [37]. For both systems, the interfacial resistance is apparently negligible, as shown by the negative intercepts in Fig. 5.

Other cases

The reduction of H_2O_2 and O_2 by a Ru(III)–histamyl complex covalently bound in a copolymer of methacrylic acid/methylacrylate is an example of Case R reaction [28]. For Case R, Koutecký–Levich plots yield $(b) = i_k^{-1} + i_p^{-1}$, as shown in Table 1. The differentiation of i_k from i_p may be accomplished by plotting (b) vs. Γ_m°; the slope is $[Fc_A^\circ \kappa k_1]^{-1}$ and the intercept is $[Fc_A^\circ \chi_f]^{-1}$. Such plots for H_2O_2 and O_2 are shown in Fig. 6, and the values found for k_1 and χ_f are summarized in Table 3. For H_2O_2, $\chi_f \to \infty$. Two values of χ_f are reported for O_2 in Table 3. A low value of 0.04 cm/s was obtained by linear regression of all five points in Fig. 6. If the point at $\Gamma^{\circ\,-1}_m = 3.45 \times 10^8$ cm^2/mol is omitted, linear regression of the remaining four points,

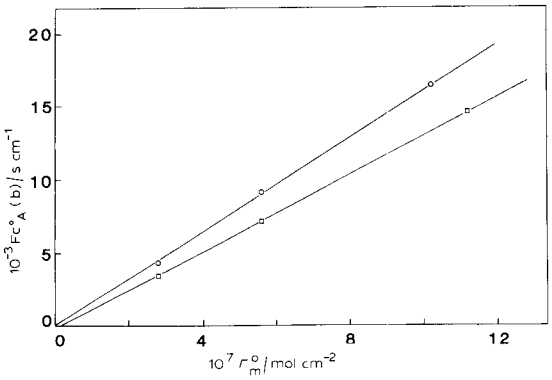

Fig. 5. Two additional plots of Fc_A° (b) vs. thickness or surface coverage for Case S. In these cases, there is no evidence of a limiting interfacial flux, as shown by the zero intercepts. Co(C$_2$O$_4$)$_3^{3-}$ through PLC (○) and Co(tpy)$_2^{2+}$ through PLC/Mo(CN)$_8^{3-}$ (□). The data was taken from refs. 29 and 37.

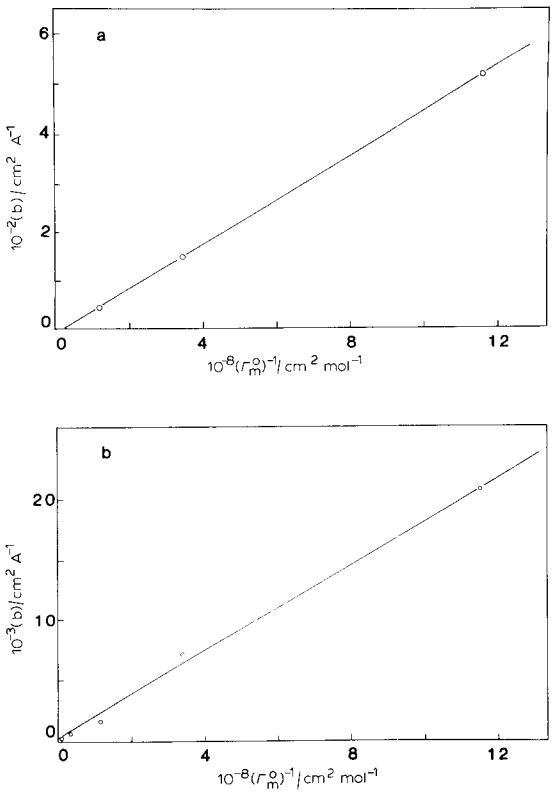

Fig. 6. Plots of intercept, (b), vs. Γ^{-1} for (a) 1.4 mM H_2O_2 and (b) saturated O_2 reduction by Ru(III)–histamyl in methacrylic acid/methacrylate copolymer. Data from ref. 28. For Case R, intercept vs. Γ^{-1} yields a slope of $[Fc_A^o \kappa k_1]^{-1}$ and an intercept of $[Fc_a^o \chi_f]^{-1}$. For 1.4 mM H_2O_2, mass transport across the interface is not an important rate limiting step, as shown by the intercept in (a). The finite intercept shown in (b) for saturated O_2 indicates the interfacial mass transfer rate may be sufficiently slow as to affect the net rate.

TABLE 3

Summary of data analysis of H_2O_2 and O_2 catalyzed by Ru(III) histamyl complex bound in a methacrylate copolymer [28]

Substrate	n [a]	χ_f/cm s^{-1}	$\kappa k_1/M^{-1}$ s^{-1} [b]	$\kappa k_1/M^{-1}$ s^{-1} [c]
H_2O_2	2	[d]	8.1×10^3	8.6×10^3
O_2	4	0.04 (0.3) [e]	10.2 (10.2) [e]	9.2

[a] Number of electrons.

[b] A finite interfacial mass transfer rate was taken into account; value calculated from the slope of the plot in Fig. 6.

[c] Value from ref. 28; An equilibrium interfacial condition was assumed.

[d] (b) vs. Γ^{-1} has a slightly negative intercept suggesting mass transport across the polymer solution interface is not a current limiting process.

[e] The value in the parentheses was determined without the point at $\Gamma^{-1} = 3.45\times10^8$ cm^2/mol.

yields a value of χ_f of ~ 0.3 cm/s. The value found for k_1 from the slope is 10% higher than the average value reported in ref. 28. Thus, there is some evidence of interfacial resistance for O_2 in this system, but the analysis is probably at the limit of statistical significance.

Murray and co-workers [17,25] examined several systems in which the cross-exchange reaction is confined to a monolayer at the polymer-solution interface. The polymers studied were poly$[Ru(VB)_3]^{2+}$ (where VB = 4-vinyl-4′-methyl-2,2′-bipyridine) [17a] and poly$[Ru(vbpy)^2]_3^+$ [17b]. The substrates used were more difficult to oxidize than the polymers; these include $[Ru(bpy)_3]^{2+}$, $[Ru(bpy)_2(4,4'\text{-}bpy)_2]^{2+}$, $[Ru(bpy)_2(py)(CH_3CN)]^{2+}$, $[Ru(bpy)_2(CH_3CN)_2]^{2+}$, and $[Ru(bpy)_2(pyrazine)_2]^{2+}$. For both polymers, the slope of the Koutecký–Levich plot for the bare and the polymer-modified electrodes were the same, and (b) was independent of Γ_m° for $10^{-9} \leq \Gamma_m^\circ \leq 10^{-8}$ mol/cm^2. Similar results were also reported in reference [25] for cobalt and copper metalloporphyrins bound to the electrode by a silane linkage. For coverages in excess of a monolayer and substrates such as $PhCHBrCH_2Br$, (b) was independent of Γ_m°. The linear Koutecký–Levich plots and the Γ_m°-independence of (b) are consistent with Case Sr + E when $i_1 \ll i_E$. Under these conditions $(b) = i_p^{-1} + i_k^{-1}$ and i_p cannot be differentiated from i_k in the monolayer case because both are directly proportional to c_A°. Thus, the reported cross exchange rates may be limited by an interfacial mass transfer component as well as by the rate of the cross exchange reaction.

DISCUSSION

The question of what factors contribute to a finite rate of interfacial mass transfer remains to be addressed. This question has been considered in non-electrochemical measurements of mass transfer across a thin polymer film suspended between two liquids. The resistance has been ascribed to a mechanical barrier [15], a hydrodynamic effect resulting from a decreased modulus of surface compressibility [16a], or suppression of eddy diffusion [16b]. MacGregor and Mahajan [13] have shown ionic repulsions account for the interfacial rate when the polymer and film have like charges. Interfacial reactions such as dimerization [16c], intercalation [12], and resolvation [15], have also been invoked to account for the second order rate.

For polymer-modified electrodes, a variety of factors could influence the interfacial mass transfer rate. As substrate molecules increase in size, i_p may decrease. Like charges on the polymer and substrate may tend to repel the substrate from the interface.

Desolvation and resolvation of the substrate when it crosses the polymer–solution interface is another process which could contribute to interfacial mass transfer resistance. The PLC is a highly solvent-swollen matrix, and the passage of $Co(tpy)_2^{2+}$ from the solution side of the polymer–solution interface to the polymer side probably proceeds without any marked change of phase, i.e., from aqueous phase to aqueous phase. However, BQ passing from MeCN solution into PVF may involve significant solvation changes.

In conclusion, the equations derived here show that the steady state solution for equilibrium mass transport across the film-solution interface are identical except i_A^{-1} is replaced by $[i_A^{-1} + i_p^{-1}]$. This implies that one additional experimental parameter, e.g., ϕ, must be varied in a known way to evaluate the rate of interfacial mass transfer. From a physical perspective, this indicates the measured current is limited by the amount of substrate arriving on the film side of the interface, whether $c_A(\phi^-)$ is determined by mass transfer in the solution or mass transfer across the interface. This theoretical outcome is a direct consequence of the steady state assumption at the solution-film interface.

ACKNOWLEDGEMENT

The support of this research by the National Science Foundation (CHE8402135) is gratefully acknowledged.

REFERENCES

1 (a) C.P. Andrieux, J.M. Dumas-Bouchiat and J.M. Savéant, J. Electroanal. Chem., 131 (1982) 1; C.P. Andrieux and J.M. Savéant, J. Electroanal. Chem., (b) 134 (1982) 163; (c) 142 (1982) 1; (d) C.P. Andrieux, J.M. Dumas-Bouchiat and J.M. Savéant, J. Electroanal. Chem., 169 (1984) 9; (e) C.P. Andrieux and J.M. Savéant, J. Electroanal. Chem., 171 (1984) 65.
2 F.C. Anson, J.M. Savéant and K. Shigehara, J. Phys. Chem., 87 (1983) 214.
3 D.A. Gough and J.K. Leypoldt, (a) Anal. Chem., 51 (1979) 439; (b) Anal. Chem., 52 (1980) 1126; (c) A.I. ChE. J., 26 (1980) 1013; (d) J. Electrochem. Soc., 127 (1980) 1278.
4 M. Delamar, M.C. Pham, P.C. Lacaze and J.E. Dubois, J. Electroanal. Chem., 108 (1980) 1.
5 C.P. Andrieux and J.M. Savéant, J. Electroanal. Chem., 111 (1980) 377.
6 C.P. Andrieux, J.M. Dumas-Bouchiat and J.M. Savéant, J. Electroanal. Chem., 114 (1980) 159.
7 N. Oyama and F.C. Anson, Anal. Chem., 52 (1980) 1192.
8 W.J. Albery and A.R. Hillman, Annu. Rep. C. (1981), The Royal Chemical Society, London, 1983, pp. 317–437.
9 R.W. Murray, Phil. Trans. R. Soc. (London) A, 302 (1981) 253.
10 R.D. Rocklin and R.W. Murray, J. Phys. Chem., 85 (1981) 2104.
11 E. Laviron, J. Electroanal. Chem., 131 (1982) 61.
12 A.J. Vaccaro, T. Palanisamy, R.L. Kerr and J.T. Maloy, J. Electrochem. Soc., 129 (1982) 682.
13 R. McGregor and I.Y. Mahajan, Trans. Faraday Soc., 58 (1982) 2481.
14 R. McGregor, Diffusion and Sorption in Fibers and Films, Academic Press, New York, 1974, p. 187.
15 J.T. Davies and J.B. Wiggill, Proc. R. Soc., A255 (1960) 277.
16 J.T. Davies and G.R.A. Mayers, Chem. Eng. Sci., (a) 16 (1961) 55; (b) 3 (1954) 248; (c) 3 (1954) 260.
17 T. Ikeda, C.R. Leidner and R.W. Murray, (a) J. Am. Chem. Soc., 103 (1981) 7422; (b) J. Electroanal. Chem., 138 (1982) 343.
18 Y. Ohnuki, H. Matsuda, T. Oshaka and N. Oyama, J. Electroanal. Chem., 158 (1983) 55.
19 D.R. Gabe, Principles of Metal Surface Treatment and Protection, 2nd ed., Pergamon Press, Oxford, 1978.
20 J.B. Kerr, L.L. Miller and M.R. Van De Mark, J. Am. Chem. Soc., 102 (1980) 3383.
21 C. Degrand and L.L. Miller, J. Am. Chem. Soc., 102 (1980) 5728.
22 A. Bettelheim, R.J.H. Chan and T. Kuwana, J. Electroanal. Chem., 110 (1980) 93.
23 I. Rubinstein and A.J. Bard, J. Am. Chem. Soc., (a) 102 (1980) 6641; (b) 103 (1981) 5007.
24 J. Facci and R.W. Murray, Anal. Chem., 54 (1980) 772.
25 R.D. Rocklin and R.W. Murray, J. Phys. Chem., 85 (1981) 2104.

26 K.K. Kuo and R.W. Murray, J. Electroanal. Chem., 131 (1982) 37.
27 G. Samuels and T.J. Meyer, J. Am. Chem. Soc., 103 (1981) 307.
28 K. Shigehara and F.C. Anson, J. Electroanal. Chem., 132 (1982) 107.
29 F.C. Anson, T. Oshaka and J.M. Savéant, J. Am. Chem. Soc., 105 (1983) 4883.
30 F.C. Anson, J.M. Savéant and K. Shigehara, J. Electroanal. Chem., 145 (1983) 423.
31 J. Leddy and A.J. Bard, J. Electroanal. Chem., 153 (1983) 223.
32 R.W. Murray, A.E. Ewing and B.J. Feldman, unpublished results; to be submitted.
33 T. Ikeda, R. Schmehl, P. Denisevich, K. Willman and R.W. Murray, J. Am. Chem. Soc., 104 (1982) 2683.
34 N. Oyama, N. Oki, H. Ohno, Y. Ohnuki, H. Matsuda and E. Tsuchida, J. Phys. Chem., 87 (1983) 3642.
35 P.C. Lacaze, M.C. Pham, M. Delamar and J.E. Dubois, J. Electroanal. Chem., 108 (1980) 9.
36 F.C. Anson, J.M. Savéant and K. Shigehara, J. Am. Chem. Soc., 105 (1983) 1096.
37 F.C. Anson, T. Ohsaka and J.M. Savéant, J. Phys. Chem., 87 (1983) 640.